MDPI

*Article*

# Mechanical Properties of Faecal Sludge and Its Influence on Moisture Retention

Arun Kumar Rayavellore Suryakumar [1,*], Sergio Luis Parra-Angarita [2,*], Angélique Léonard [2], Jonathan Pocock [1,3] and Santiago Septien [1]

1 WASH R&D Centre, University of KwaZulu-Natal, Durban 4000, South Africa; pocockj@ukzn.ac.za (J.P.); septiens@ukzn.ac.za (S.S.)
2 Chemical Engineering Research Unit, PEPs, University of Liège, 4000 Liège, Belgium; a.leonard@uliege.be
3 Department of Chemical Engineering, University of KwaZulu-Natal, Durban 4000, South Africa
* Correspondence: 220112475@stu.ukzn.ac.za or rsarunkumar@gmail.com (A.K.R.S.); slparra@uliege.be (S.L.P.-A.)

**Abstract:** The mechanical properties of faecal sludge (FS) influence its moisture retention characteristics to a greater extent than other properties. A comprehensive fundamental characterisation of the mechanical properties is scarcely discussed in the literature. This research focused on bulk and true densities, porosity, particle size distribution and zeta-potential, extracellular polymeric substances, rheology and dilatancy, microstructure analysis, and compactibility in the context of using the FS as a substitute for soil in land reclamation and bioremediation processes. FSs from different on-site sanitation systems were collected from around Durban, South Africa. The porosity of the FSs varied between 42% and 63%, with the zeta-potential being negative, below 10 mV. Over 95% of the particles were <1000 μm. With its presence in the inner part of the solid particles, tightly bound extra-cellular polymeric substances (TB-EPSs) influenced the stability of the sludge by tightly attaching to the cell walls, with the highest being in the septic tank with the greywater sample. More proteins than carbohydrates also confirmed characterised the anaerobic nature of the sludge. The results of the textural properties using a penetrometer showed that the initial slope of the positive part of the penetration curve was related to the stiffness of the sludge sample and similar to that of sewage sludge. The dynamic oscillatory measurements exhibited a firm gel-like behaviour with a linear viscoelastic behaviour of the sludges due to the change in EPSs because of anaerobicity. The high-TS samples exhibited the role of moisture as a lubricating agent on the motion of solid particles, leading to dilatancy with reduced moisture, where the yield stress was no longer associated with the viscous forces but with the frictional contacts of solid–solid particle interactions. The filtration–compression cell test showed good compactibility, but the presence of unbound moisture even at a high pressure of 300 kPa meant that not all unbound moisture was easily removable. The moisture retention behaviour of FS was influenced by its mechanical properties, and any interventional changes to these properties can result in the release of the bound moisture of FS.

**Keywords:** porosity; particle size distribution; zeta potential; extracellular polymeric substances; compactibility; microscopy imagery

## 1. Introduction

With over 70% of the households in the developing world relying on non-sewered sanitation systems, faecal sludge (FS) treatment is a pivotal step in containing land and

water degradation. Faecal sludge management is therefore a primary measure to treat this biohazard and pave a way to reuse the significant nutrients and organics beneficially [1,2]. FS is fundamentally challenging because of its variability and unpredictability, and it is scientifically poorly understood [3]. The mechanical, physicochemical, and bio-chemical properties of FS are varied and complex, and it is difficult to summarise its characterisation [4]. The association of moisture in the sludge makes it more complex, and hence, one of the important stages of treatment of FS is solid–liquid separation. This stage of treatment helps with substantial volume reduction, wherein both the solid and liquid fractions can be treated separately with better effectiveness and efficiency [5].

With moisture associated with the solid particles in sludge constituting unbound moisture and bound moisture, the separation of moisture from the solids in sludge is not simple. Besides factors like the type of on-site sanitation system used and the quantity of water used in toilets, different properties of the sludge influence solid–liquid separation [6,7]. With a mix of microorganisms, colloids, and particles of different origins, the extreme variability of FS adds another difficult dimension of complexity [8]. Analysis of these properties of sludge helps to understand the complex moisture retention behaviour of the sludge. Further, the design of solid–liquid separation technologies requires the characteristics of sludge for efficient operations.

The initial stage of this research distinguished the four categories of moisture associated with sludge solids (unbound moisture, interstitial moisture, vicinal moisture, and intracellular moisture) and their proportions by different instrumentation methods. The focus of this paper is to provide the fundamental characteristic data and a relatively comprehensive analysis of the mechanical properties of faecal sludge in the context of its moisture retention behaviour [9]. The need for the reuse of treated FS is gaining momentum, with a particular focus on land applications. The determination of the mechanical properties will help in understanding the moisture and nutrient retention behaviour, its compactibility in the natural environment, and its use as a substitute for soil in land reclamation and bioremediation in the context of circular economy. A complete database of the engineering behaviour of FS is therefore necessary, and the minimum properties needed include the bulk and true densities, porosity, particle size distribution (PSD) and zeta-potential (ZP), extracellular polymeric substances (EPSs), rheology and dilatancy, microstructure analysis, and compactibility. PSD helps determine the settleability of the sludge particles, while ZP indicates surface charge and electrostatic repulsion to floc formation. EPSs and their fractions hold moisture, and its quantification directly indicates the solid–liquid separability behaviour of sludge. The rheological behaviour of sludge is important for defining the sludge structurally, considering the interactions of sludge particles, moisture, and air. The higher the solid–liquid separability, the more stable the sludge and hence, the better for land applications [10].

Comprehensive studies on the mechanical behaviour of FS are scarce in the literature. Information does exist on sewage sludge and other industrial sludges. This study henceforth examines the mechanical properties of FS and thus adds to the next layer of circularity, addressing the need to investigate the properties that influence and/or are influenced by the solid–liquid separability of FS [11].

## 2. Materials and Methods

### 2.1. Source of Samples

Faecal sludge for the research originated from different on-site sanitation systems prevalent in different regions and countries across Africa and Asia. The samples were collected from the peri-urban areas of eThekwini municipality, Durban, South Africa, and Pietermaritzburg, South Africa. The three types of faecal sludge were:

1.  Faecal sludge from ventilated pit latrines (VIPs);
2.  Faecal sludge from urine diversion dehydrating toilets (UDDTs);
3.  Faecal sludge from septic tanks (ST) (also referred to as septage)
    a.  With grey water (ST-wGW);
    b.  With only black water (ST-BW).

The VIP samples were collected from two latrines not desludged for at least 5 years. The UDDT samples were taken from the dehydrating vault of the UDDT, with an estimated sludge storage of 15–18 months. The septic tank (ST) samples were collected from desludging vacuum tanker trucks, and composite samples were taken from septic tanks that are connected only to the toilets (ST-BW) and the ones connected to all the wastewater flow (ST-wGW). The two ST samples represent both the African and South Asian types of STs. The desludging interval of STs is usually less than a year for ST-wGW and 4–6 years for ST-BW.

VIP, UDDT, and ST-wGW samples were collected from eThekwini municipality, Durban, and ST-BW samples from Pietermaritzburg. All the samples were collected in lined plastic containers with air-tight lids, screened for trash and debris, and stored in the cold room at the laboratory at 4 °C to avoid microbial degradation and to minimise any loss in moisture. All the samples were analysed for total solids (TSs), volatile solids (VSs), pH, and electrical conductivity (EC) at the time of sampling, and these parameters were monitored for any change during the experimental period. The acceptable range of variation in the parameters was found to be <2%.

*2.2. Experimental Methods*

2.2.1. Density

The true density was determined using an Ultrapyc foam gas pycnometer (Anton Paar, Warszawa, Poland). Samples were dried in a ventilated oven for 12 h at 51 °C and kept in a desiccator before performing the analysis. The measurement settings applied were as follows: gas—helium; target pressure—18.0 psi; flow direction—sample first; target temperature—20 °C; flow mode—monolith; cell size—medium, 45 cm$^3$.

The porosity of the sludges was determined by the equation:

$$P(\%) = \left(1 - \frac{\rho_b}{\rho_t}\right) \times 100 \tag{1}$$

where P is the porosity as a percentage, and $\rho_b$ and $\rho_t$ are the bulk density and true density in g/cm$^3$, respectively. The bulk density of the samples was determined by Archimedes' principle by measuring the volume of water displaced by a known mass of the sample [12].

2.2.2. Particle Size Distribution and Zeta Potential Measurements

The PSD and ZP were determined using a Zetasizer Nano ZS (Malvern Instruments Corp, Worcestershire, UK). The measurement of the angular variation of scattered light when a laser beam is passed through the dispersed particulate matter provided the PSD of the sample. The angular scattering intensity data were analysed to calculate the particle size [13]. All the samples were diluted using distilled water to generate suitable scattering intensity. The dilution was important for avoiding multiple reflections and measuring proper values of laser light obscuration. One mL of the sample was transferred using a micropipette into the 10 mm-diameter 40 μL disposable polystyrene cuvettes. The refractive index of the dispersant (water) and the sludge particles was 1.330 and 1.520, respectively. The DLS approach yielded the hydrodynamic diameter and the polydispersity index (PI) as a measure of PSD. The mean diameter was obtained by calculating the average of three measurements. All the experiments were conducted at 25 °C [14].

The Zetasizer uses laser Doppler velocimetry to determine the electrophoretic mobility. The experiments were conducted at 25 °C in 40 μL polystyrene cuvettes with a path length of 10 mm using water as a dispersant. Measurements were performed in triplicate and by diluting the samples in 10 mL of distilled water.

### 2.2.3. Measurement of EPSs and Total Organic Carbon (TOC)

EPSs are composed of many organic substances, mainly proteins, polysaccharides, humic acids, and little fractions of lipids, nucleic acids, and amino acids. EPSs, which exist outside the cells, are further divided into loosely bound EPSs (LB-EPSs) and tightly bound EPSs (TB-EPSs) and can be generally separated by centrifugation [15,16].

#### 2.2.3.1. Extraction of EPSs

There is no standard method for the extraction of EPSs and their fractions—LB-EPSs and TB-EPSs. They can be extracted by different physical and chemical methods. Many methods involve thorough washing, preceded by harsh extraction, which measures total EPSs or TB-EPSs. LB-EPSs are known to influence sludge floc structure, and hence measurement of it is as important as that of TB-EPSs. Hence, in this research, the EPS and its fractions were extracted from the FS samples by adopting a two-step heat extraction (mild step and harsh step) method. The mild extraction step yielded LB-EPSs, while the harsh extraction step was to extract TB-EPSs from the sludge suspension [17–19]. The method involved centrifuging the sample in a 50 mL centrifugal tube at 4000 rpm for 5 min, discarding the supernatant, resuspending the sludge pellet in a 0.05% NaCl (*w/v*) warm solution at 50 °C, and shearing it using a vortex mixer for 1 min. The suspension was then centrifuged at 4000 rpm for 10 min, and the organic matter in the supernatant was regarded as LB-EPS. For TB-EPS, the sludge pellet was resuspended again in 0.05% NaCl solution, and this suspension was heated in a water bath for 30 min at 60 °C. Post heating, the suspension was centrifuged at 4000 rpm for 15 min, and the supernatant liquid was regarded as TB-EPS. The cell lysis was said to be of no significance after this extraction process [20].

#### 2.2.3.2. EPS—Protein and Carbohydrate Determination

Since proteins and carbohydrates form the major components of EPSs, measurement of proteins and carbohydrates of the extracted fractions was carried out. For the measurement of proteins, measuring amino acids gives an accurate approximation of the proteins present. However, due to cost and time considerations, total nitrogen is widely used to estimate crude protein content [21]. In this research, the nitrogen was determined by the nitrogen combustion method, and the protein content was calculated from the nitrogen measurement.

Elemental analysis of nitrogen, along with carbon and sulphur, was quantified in the multi-element combustion CNS analyser Leco CNS 2000 (Leco Corporation, St. Joseph, MI, USA). Fitted with an auto-sampler, the CNS analyser was heated up to 1450 °C in a pure oxygen environment, with 1–2 g of sample placed in the oven in a ceramic boat.

Crude protein percent (CP%) [22] was provided by

$$\%CP = \%N \times F \tag{2}$$

where *F* is 6.25 (from 6.25 g proteins per g N).

The total carbohydrates, including mono-, di-, oligo-, and polysaccharides, was analysed by the phenol–sulphuric acid method [21]. All experiments were carried out in triplicate.

The total organic carbon (TOC) was determined by the standard operating procedure, involving chemical oxidation of the sludge samples using sulphuric acid, potassium

dichromate, and mercuric sulphate. The reduced chromium was measured at 590 nm in the spectroquant [23].

### 2.2.4. Penetrometer Test

Penetration tests and texture profile analysis (TPA) were conducted using an LS1-302 penetrometer universal traction machine (Ametek Lloyd instruments, Hampshire, UK) equipped with a 10 N probe and a 30 mm-diameter spherical geometry probe. FS samples weighing 60 g were placed in an aluminium capsule and penetrated to a depth of 15 mm at a constant speed of 1 mm/s, and the load phase (compression) and a discharge phase (relaxation) were included [24,25]. This setup simulated the practical conditions FS might encounter during handling and processing.

### 2.2.5. Rheology and Dilatancy

FS exhibits viscoelastic properties, blending the characteristics of both solids and liquids, thereby exposing the traits of viscosity and elasticity when subjected to stress or deformation. An oscillatory experiment such as an amplitude sweep can be conducted to measure these changes in rheology. Dynamic rheological measurements were carried out using Anton Paar Physica MCR 302 (Anton Paar Benelux, Gentbrugge, Belgium) in the chemical engineering laboratory at the University of Liege, Belgium. The instrument was a piece of controlled stress rheometer equipment with a 50 mm parallel plate geometry. The gap between the fixed plate and the oscillating plate was fixed at 2 mm. The samples were homogenised before being added to the plate on the rheometer at a temperature of 20 °C.

The samples were submitted to a frequency sweep from 0.1 to 100 rad/s at a constant shear strain in the linear viscoelastic region, and the strain sweep experiments were conducted from 0.01% to 10%. Each measurement was performed in triplicate. The elastic modulus or storage modulus $G'$ characterised the energy stored in elastic form and was retrievable by the sample (elastic component), while the viscous modulus or loss modulus $G''$ characterised the energy lost by friction (viscous component), and are given by:

$$G' = G^* \cos \delta \tag{3}$$

$$G'' = G^* \sin \delta \tag{4}$$

where the complex viscoelastic modulus $G^*$ is defined as the ratio of the amplitudes stress and strain. The $G'$ and $G''$ were present in the results, which were the function of the frequency [26].

Mouzaoui [27] developed a specific procedure to determine dilatancy by considering the edge effects and measuring the normal force simultaneously with the tangential shear stress using a rotational rheometer. Samples with different TSs of VIP and UDDT sludge ranging from 10% to 43% were prepared with dilution (low TS) and centrifugation (high TS). The rheological investigations were carried out at IMT-Mines, Albi, France, with a stress-controlled RS600 HAAKE Rheostress 600 instrument (Thermo Fisher Scientific, Karlsruhe, Germany), and the RheoWin Pro Job Manager software (Version 3.61) was used to assist with data analysis. Serrated parallel plates of 35 mm diameter were used, with a gap of 2 mm. For different TS concentrations, a stress sweep was applied to the sample, which consisted of successive steps of constant dynamic stress of increasing intensity. A pause was marked between each step as a reference to allow for the correction of edge effects (fractures and cracks). Thus, by applying a constant dynamic rotational angle, the edge effects were reduced in accordance with the corresponding stress. Tests were conducted in triplicate to evaluate reproducibility, and normal force was recorded along with the tangential shear stress.

### 2.2.6. Filtration–Compression Test

A lab filtration device at the Environmental Engineering laboratory, Cranfield University, United Kingdom, designed to carry out permeability and compressibility tests, was adapted for compactibility experiments. Experiments were carried out for two of the four FS samples—VIP and ST-BW—thus representing both the high-TS sample and the low-TS sample. The device consisted of a compressive piston moving in a 40 mm-diameter cylinder with a depth of 120 mm. At the bottom of the chamber, a filter paper (Fisherbrand of porosity 0.6 µm) was placed on a perforated disk. A stepped pressure was applied to the piston, controlled by a program-based regulating system. The pressure steps were at 0.2 bar, 0.5 bar, 1.2 bar, and 3 bar.

Raw FS samples of approximately 50 g $\pm$ 3 g were added to the cylindrical vessel without any change in the initial characteristics. The piston was firmly placed in the cylinder to avoid any air gaps. The pressure system was started, and the filtrate was collected in a tray. The loss of moisture was measured continuously by data-logging software connected to the device. The test duration extended to up to 3–7 days depending on the type of FS sample. After the completion of the test, the moisture content of the sample cakes was measured as per standard methods [28]. Thermogravimetric analysis (TGA) was carried out for all the samples before and after the compaction tests. The analysis was carried out using pure $N_2$ as the carrier gas at a flow rate of 10 mL/min, with 35–40 mg of samples, and the cell temperature increased from ambient (27°C) to 90 °C at a rate of 10 °C/min and was maintained at 90 °C in isothermal conditions for 45 min using a TGA8000 (Perkin Elmer, Waltham, MA, USA) [29,30].

### 2.2.7. Microscopic Observations

While scanning electron microscopy (SEM) is widely used in various fields such as material sciences, geology, and biology for providing direct characterisation of the microstructure of the materials, the sample must be completely dried. Environmental scanning electron microscopy (ESEM) is an advanced SEM capable of maintaining the integrity of the sample at a range of different relative humidities. Hence, the micrographs from ESEM are more representative of the microstructure of the sample [31]. Observations were conducted with ESEM to explore the surface morphology of the FS. The Philips XL-30 ESEM-FEG (FEI Company, Hillsboro, OR, USA) was capable of imaging any sample, including wet samples, which was the pre-requisite for imaging raw FS samples. No changes were made to the samples. The samples were analysed at an acceleration voltage of 10 kV and a magnification of up to 12.8 kX.

## 3. Results and Discussion

### 3.1. Densities and Porosity

Bulk density is defined as the ratio of a sample's mass to its bulk or macroscopic volume, including pore spaces. Usually expressed in grams per cubic centimetre, bulk density conforms the accepted physical terminology. True density was determined by the gas pycnometer and porosity was calculated as per Equation (1). Table 1 contains the results for the bulk and true densities and the porosity. The bulk density of the UDDT sample was significantly higher than that of the other FS samples due to the lower initial moisture content.

**Table 1.** Densities, porosity, particle size distribution, and zeta potential of FSs.

|  | FS Samples | | | |
|---|---|---|---|---|
|  | **VIP** | **UDDT** | **ST-wGW** | **ST-BW** |
| Bulk density g/cm$^3$ | $0.97 \pm 0.02$ | $1.14 \pm 0.03$ | $0.83 \pm 0.01$ | $0.94 \pm 0.01$ |
| True density g/cm$^3$ | $1.96 \pm 0.03$ | $1.80 \pm 0.05$ | $1.92 \pm 0.04$ | $1.71 \pm 0.06$ |
| Porosity % | $48.94 \pm 1.46$ | $62.70 \pm 1.93$ | $42.48 \pm 1.78$ | $54.33 \pm 1.32$ |
| PS < 10 μm % | $19.98 \pm 1.31$ | $20.21 \pm 1.12$ | $18.68 \pm 0.79$ | $13.94 \pm 0.48$ |
| PS 10–100 μm % | $39.51 \pm 2.76$ | $42.38 \pm 1.99$ | $60.28 \pm 2.48$ | $54.02 \pm 2.81$ |
| PS 100–1000 μm % | $34.82 \pm 1.11$ | $32.93 \pm 0.97$ | $21.04 \pm 0.52$ | $31.78 \pm 0.69$ |
| PS > 1000 μm % | $5.68 \pm 0.02$ | $4.47 \pm 0.01$ | $0.00 \pm 0.01$ | $0.25 \pm 0.01$ |
| ZP mV | $-17.10 \pm 0.88$ | $-17.30 \pm 0.42$ | $-10.25 \pm 0.22$ | $-12.90 \pm 0.37$ |

*3.2. Particle Size Distribution (PSD)*

Colloidal and supra-colloidal particles affect the settleability of sludge particles; hence, knowing the amounts of particles present in the sludge according to the sludge's size is important. Different sizes of sludge particles influence the sludge's moisture retention characteristics. The smaller the particle size, the harder the solid–liquid separability because of the higher specific surface, which binds more moisture per volume fraction. Smaller particles have lower settling velocities and hence retain more moisture [32]. PSD characterisation of aerobic sewage sludges is typically unimodal, and its maximum is towards the larger particles. The particle sizes of sewage sludge from aerobic treatment facilities varied from 0.3 μm to 310 μm, with the largest fraction of over 60% in the range of 50–60 μm and the lowest range from 0.40 μm to 2.59 μm. Approximately 90% of the particles did not exceed 140 μm in the sewage sludge. The presence of some colloidal particles of a size <1 μm influenced the solid–liquid separability [14,33].

On the contrary, the primary PSDs of the FS samples were mainly distributed in the range of 10–1000 μm, with 20% of the particles <10 μm, 40–60% in the range of 10–100 μm, 21–34% in the range of 100–1000 μm, and <5% > 1000 μm (Figure 1). The high-TS samples of VIP and UDDT had a similar distribution, while both ST samples were similar to each other, indicating the possible role of greywater and other contaminants. All the samples had relatively uneven but similar distributions. Further, the literature says that the flocs are fragmented under anaerobic conditions; hence, the FSs, which were primarily anaerobic sludges, had reduced particle sizes that were fragmented. Over 95% of the particles were less than 1000 μm for the UDDT and VIP sludges, and for the ST sludges, particles <1000 μm constituted up to 99% of the sample. This reduced particle size resulted in low settleability, which was evident in the batch-settling tests carried out for the same samples [34] (under review). However, the presence of increased specific surface area can influence solid–liquid separability positively with the addition of an appropriate coagulant [35].

*3.3. Zeta Potential*

The surface charge of the sludge particles provides the sludge's agglomeration behaviour, i.e., its ability to coagulate and release moisture. The value of ZP indicates the dispersion behaviour of the sludge. ZP is used to characterise the positive and negative charges on the surface of materials and the electrostatic repulsion, which prevents them from accumulating and thereby resulting in the sediment gaining mass. The ZP of all the samples was negative, indicating that all FSs were negatively charged. While the high-TS samples had higher values of ZP, the lower-TS samples had ZP values similar to those of sewage sludges. Particles with a ZP between –30 mV and +30 mV tend to release vicinal

moisture on the surface of the sludge particles upon addition of a coagulant. The closer the ZP value is to its isoelectric point when ZP equals zero mV, the easier it is to coagulate [36].
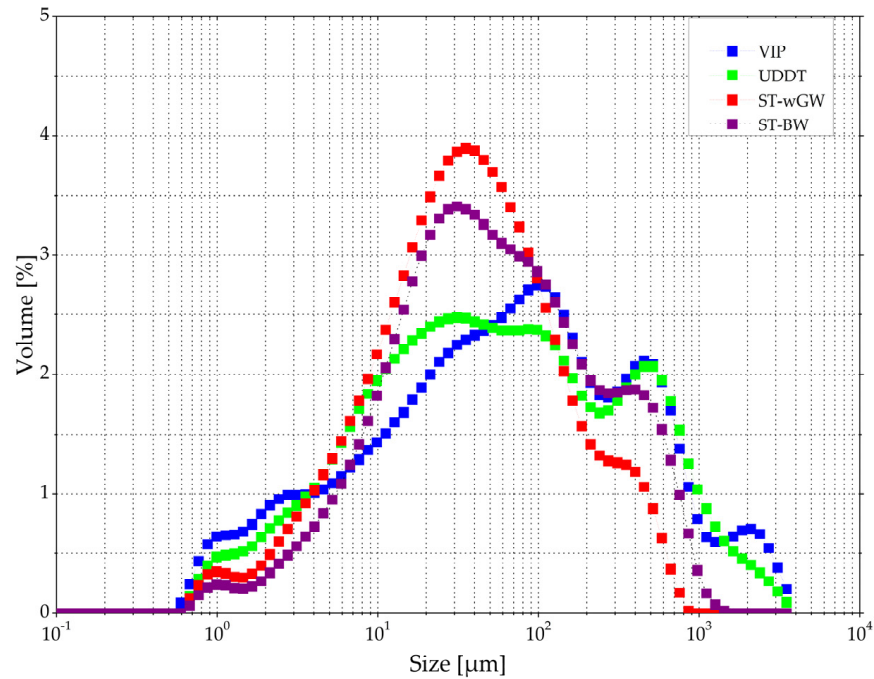


**Figure 1.** Particle size distribution of all FSs.

The heat map of the PSD and ZP (Figure 2) provided the correlatability between fractions of the PSD and ZP. Analysing the correlation between PSD and ZP using Python, it was found that ZP was positively correlated with the percentage of particles between 10 and 100 μm. A correlation value of 0.87 indicated strong positive correlation. The higher the lower-diameter particles, the higher and more negative the ZP.
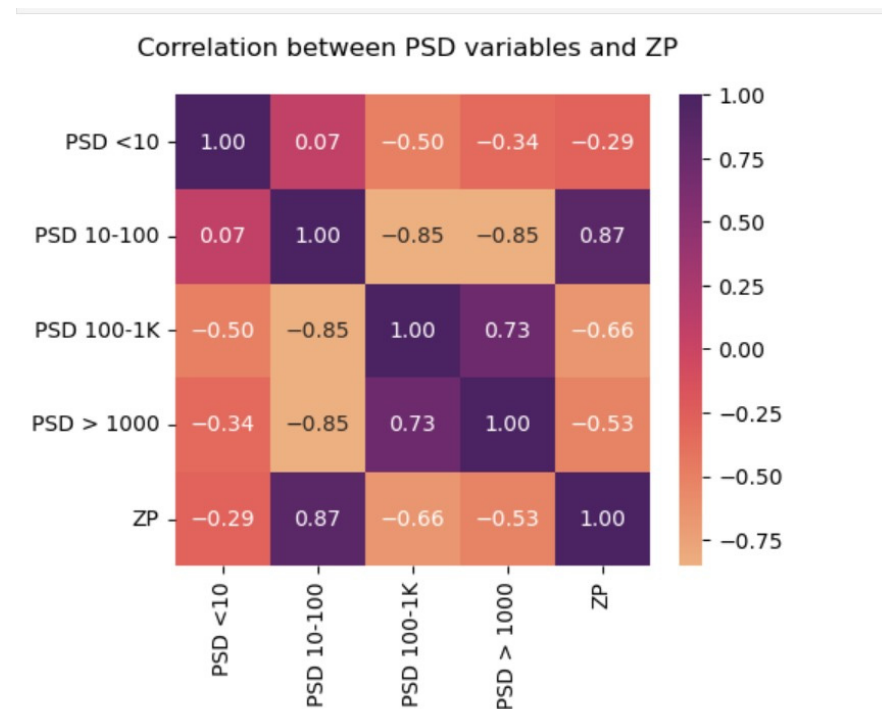


**Figure 2.** Correlation between PSD and ZP.

ZP was negatively correlated with the percentage of particles <10 μm, between 100 and 1000 μm, and >1000 μm. The relationship between PSD size ranges (in μm) and ZP (mV) can be given by Equation (3):

$$ZP = -34.34 - (0.12 \times PSD < 10) + (0.44 \times PSD10{-}100) + (0.4 \times PSD > 1000) \qquad (5)$$

*3.4. Extracellular Polymeric Substances*

Though by definition interstitial moisture is simply the moisture trapped between sludge particles, it is evident that there are some weak forces acting on interstitial moisture. A significant fraction of moisture is held by a polymer-like network with a presence of large concentrations of counter-ions. Extracellular polymeric substances (EPSs) are secreted by bacteria primarily to protect the solid biomass in the sludge from the external environment. Though their exact role is not completely understood, EPSs are characterised by high moisture, which makes it difficult to unpack the solid aggregates, thereby leading to a hydrated state of moisture retention. EPSs form a significant fraction of this sludge mass. EPSs are such a critical property of FS because they influence the physicochemical behaviour of the sludge and thus affect its moisture retention by providing electrostatic interactions and hydrogen bonds. EPSs are one of the most influential substances in terms of the moisture retention characteristics of sludge because of their cross-linking polymeric network-like structure [37]. They are composed of many organic substances, mainly proteins, polysaccharides, humic acids, and little fractions of lipids, nucleic acids, and amino acids, with proteins and polysaccharides as the main fractions [16]. Because of their complexity and importance, EPSs are extensively researched, specifically in solid–liquid separability of sludges. This is because EPSs form a complex three-dimensional sludge matrix-like structure [38]. EPSs in the sludge matrix typically form a double-layered structure, consisting of loosely bound EPSs (LB-EPSs) and tightly bound EPSs (TB-EPSs). LB-EPSs are said to be diffused from TB-EPSs and function as a surface for cell attachment. This classification of EPSs is based on the extraction methodology [18]. The role of proteins and carbohydrates in EPSs is also significant for the solid–liquid separability. The ratio of $EPS_{carb}$ to $EPS_{prot}$ is a good indicator of the moisture retention properties [35].

Further, most on-site sanitation systems, such as septic tanks and pit latrines, in non-sewered sanitation are anaerobic. Anaerobic atmospheres affect EPSs and were reported to have a significant impact on biosolid structure. This study analysed the dynamics of EPSs and the various sludge characteristics from the different type of on-site sanitation systems. This helped determine the effect of the extent of anaerobicity on EPSs. Within EPSs, the $EPS_{carb}$-to-$EPS_{prot}$ ratio was analysed to investigate its effect on moisture retention.

The results of the measurement of the EPSs are shown in Table 2. TB-EPSs had a significant impact on the stability of the sludge, and UDDT and ST-wGW sludges had the highest stability, also indicated by their VS/TS value. The high TB-EPSs in ST-wGW can also be attributed to the other substances present, such as soaps and oils. Further, the carbohydrate-to-protein ratio was high in the ST samples and lowest in the UDDT sludge. Further, the carbohydrate content was significantly higher than that of the proteins, attributed to the anaerobicity of the sludges [39], whereas in sewage sludges, the proteins were higher than the carbohydrates. It is also argued that anaerobically digested sludges have increased EPSs and hence have higher moisture retention [40]. More research is necessary, specifically with anaerobic sludges from OSS, to correlate the anaerobic transformations with the binding strength and the roles of shifting particle sizes and changing EPSs.

**Table 2.** EPS—crude protein and carbohydrate measurements of FSs.

| | VIP | UDDT | ST-wGW | ST-BW |
|---|---|---|---|---|
| LB-EPS—protein g/gDM | $0.99 \pm 0.07$ | $0.26 \pm 0.07$ | $6.80 \pm 0.54$ | $3.90 \pm 0.91$ |
| TB-EPS—protein g/gDM | $0.54 \pm 0.09$ | $0.74 \pm 0.27$ | $14.47 \pm 1.04$ | $2.78 \pm 0.21$ |
| LB-EPS—carbohydrates-g/gDM | $84.03 \pm 2.63$ | $93.65 \pm 3.21$ | $326.68 \pm 37.91$ | $305.88 \pm 21.56$ |
| TB-EPS—carbohydrates-g/gDM | $136.70 \pm 3.71$ | $177.27 \pm 16.20$ | $360.46 \pm 26.19$ | $328.73 \pm 28.68$ |
| Prot:Carb ratio | 144.17 | 348.82 | 32.31 | 94.92 |
| Total organic carbon (TOC) g/gDM | $927.44 \pm 2.81$ | $784.36 \pm 36.26$ | $1656.05 \pm 177.14$ | $1389.67 \pm 101.20$ |

From the correlational analysis between TOC and EPSs (Figure 3), TOC was positively correlated to proteins and carbohydrates, both loosely bound and tightly bound, with the correlation with LB-EPS$_{carb}$ the highest at 0.87. TB-EPS$_{prot}$ was strongly correlated to LB-EPS$_{prot}$ but least correlated to TOC. Both LB-EPS$_{carb}$ and TB-EPS$_{carb}$ showed strong positive correlation with LB-EPS$_{prot}$.
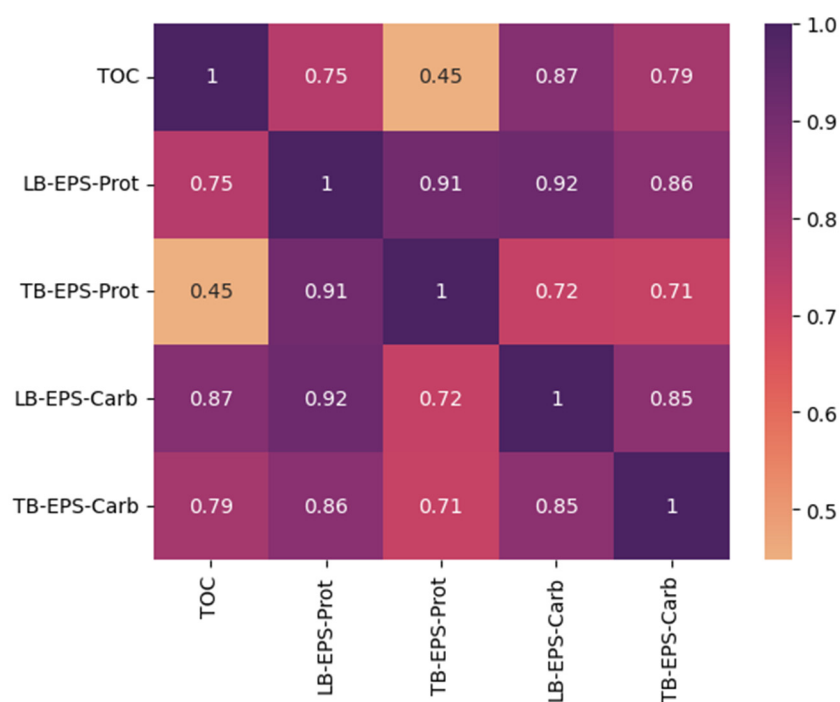


**Figure 3.** Correlation of TOC with EPSs.

### 3.5. Penetration Curve

The application of a ball penetrometer was carried out to investigate the cohesiveness and adhesiveness of the FS samples. During the penetration of the ball in the sample, the surrounding sample undergoes shear strains and softens, and a certain extent of the softening is measured in the resistance [41]. In Figure 4, the schematic penetration curve for faecal sludge (FS) is presented. In this graph, the maximum positive peak (Fmax in N) represents the force required for the probe to penetrate the sample to its maximum depth. Fmax is commonly associated with the firmness or hardness of the sample. The positive area under the curve up to Fmax (A+ in mJ/Nmm) reflects the work performed by the probe during the compression test on the sample [42]. For high-TS sludges, adhesion and cohesion strengths were no longer the same due to the lower moisture content. The shearing stress of adhesion reached a maximum, whereas the shearing stress of cohesion continued to rise, which indicates that the resistance between the sludge and the probe

was smaller than the internal resistance of the solid–solid and solid–liquid particles. This explains the increase in stickiness of the sludge as moisture was removed [43].
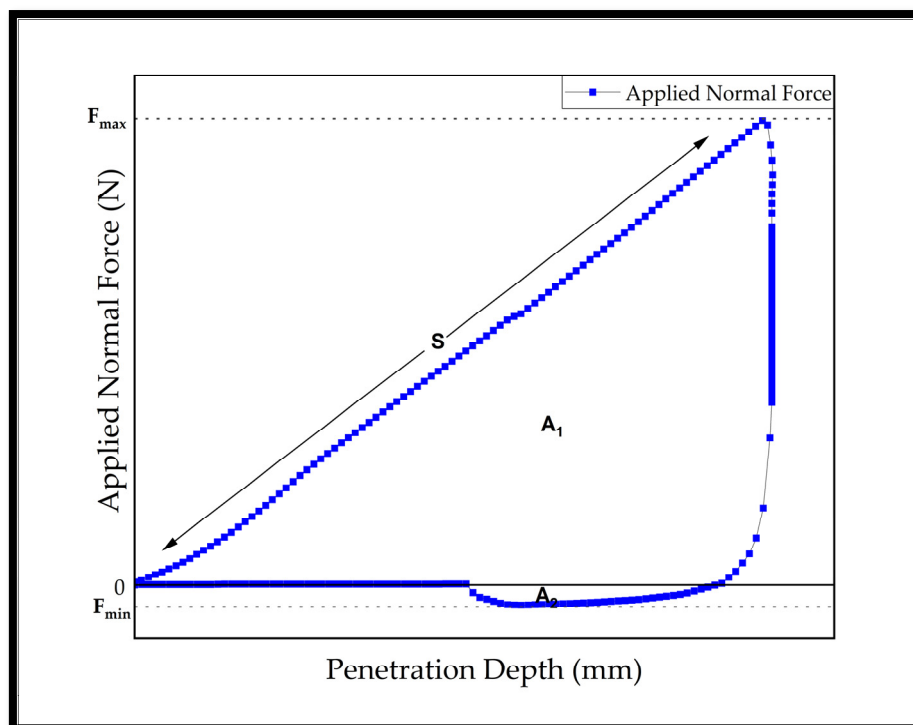


**Figure 4.** Experimental penetration curve.

The minimum negative peak (Fmin in N) corresponds to the force needed to detach the sample from the probe and is defined as the adhesive force of the sample. The more negative the Fmin value, the greater the adhesion. The negative area under the curve ($A_1$, in mJ/Nmm) represents the work required to separate the probe from the sample, acting as an indicator of adhesiveness, stickiness, or tackiness (i.e., the energy needed to remove the sample from surfaces) [44,45].

The initial slope of the positive part of the penetration curve (S in N/mm) is related to the stiffness of the sludge sample [46]. Finally, the cohesive load of the sample was obtained from the maximum load recorded (in kPa) when the probe penetrated the sample [24,47]. The mean values of the textural properties for the FSs, calculated from three measurements, are provided in Table 3.

**Table 3.** Textural properties of FSs.

| Variable | Property | Units | VIP | UDDT |
|:---:|:---:|:---:|:---:|:---:|
| Fmax | Hardness | N | $1.4 \pm 0.11$ | $1.3 \pm 0.10$ |
| Fmin | Adhesive force | N | $-0.39 \pm 0.02$ | $-0.34 \pm 0.03$ |
| S | Rigidity | N/mm | $0.1 \pm 0.01$ | $0.1 \pm 0.01$ |
| $A_1$ | Hardness work performed | N·mm | $8.8 \pm 0.66$ | $7.8 \pm 0.82$ |
| $A_2$ | Adhesiveness | N·mm | $-3.6 \pm 0.11$ | $-3.5 \pm 0.58$ |
| - | Cohesive load | kPa | $1.04 \pm 0.08$ | $0.96 \pm 0.07$ |

Although the mean values for the textural properties of FS are not widely reported in the literature, the results of this study on FS samples do not compare to the same magnitude as those reported for sewage sludge samples before their hydration nor align with those

reported for poorly flocculated sewage sludge samples [48,49]. The cohesiveness of the FS samples analysed in this study was between 10 and 100 times lower than that reported for flocculated and dehydrated sewage sludge processed by filtration under optimal conditions. The adhesiveness of the FS samples was 5 to 10 times greater than that of sewage sludge [24]. This suggests that while FS could be directly applied in agricultural settings and for land bioremediation, it lacks the structural stability needed for storage in piles and tends to adhere easily to tools and machinery, thereby complicating its handling. This issue can be mitigated operationally by incorporating a texturising agent—such as sawdust, dry sludge, etc.—that can absorb moisture (unbound and interstitial) and provide structural support to facilitate material handling [50–53].

*3.6. Rheology and Dilatancy*

The rheological characterisation of FS provides valuable quantitative parameters that describe its complex, flexible structure, which arises from the interaction of its three main components—solid particles, moisture, and air. The forces between these components define the molecular structure and the solid–moisture framework. FS behaves as a soft, viscoelastic, non-Newtonian fluid with non-constant viscosity; this gel-like material does not transition into a liquid state and exhibits significant resistance to flow, which varies with its moisture content [54]. Specifically, the non-Newtonian properties of sludge intensify as unbound moisture decreases and bound moisture increases. Understanding the rheological behaviour of FS, influenced by both its initial and its bound moisture content, is essential for predicting its solid–liquid separability [55]. To characterise the viscoelasticity of FS, two fundamental parameters of dynamic rheology were applied—the elastic modulus or storage modulus ($G'$) and the viscous modulus or loss modulus ($G''$).

Most studies on the rheological behaviour of FS have focused on its unbound moisture phase, specifically at low to moderate total solid (TS) concentrations of between 1% and 5%. The Herschel–Bulkley model has commonly been applied to describe the yield stress and flow curve behaviour in these low-TS sludges [42].

However, in sludges with a higher TS content, FS exhibits a solid-like behaviour at rest that deforms under applied force and retains this deformed state after the force is removed. This behaviour results from the interactions between the sludge's components, which forms microstructures that, while initially resistant to deformation, eventually break up and flow under applied force [56].

For more concentrated FS samples, classical oscillatory rheology has been used effectively to study their behaviour, yielding consistent and reproducible results by managing crack and fracture formation [27]. The method used to measure the rheological properties in this study is particularly useful for samples with a TS content of between 20% and 45%, representing the interface between unbound and bound moisture zones. As TS content increases, the sludge transitions from an elastic to a plastic regime, allowing for the assessment of dilatancy.

Dilatancy, a phenomenon first described by Reynolds in 1885, is defined as the tendency for densely packed hard particles to expand perpendicularly to the shear plane when subjected to shear. In simpler terms, as particles tightly packed together exert force on neighbouring particles during motion, a normal force arises simultaneously with tangential shear stress, initiating movement in adjacent particles [27].

Figure 5 presents a schematic of the results from amplitude sweeps, or a rheogram, showing three distinct regions: viscoelastic, transition, and flow. Each of these regions is defined by specific shear strain limits. In all the samples studied, $G'$ and $G''$ remained nearly constant at low strain levels, thus displaying a linear viscoelastic, gel-like behaviour. As strain increased and the FSs reached their viscoelastic limit or yield stress ($\gamma_L$), $G'$ began

to decrease significantly, while $G''$ continued rising to a peak before starting to decline. According to the literature on sewage sludges, higher TS content expands in the linear viscoelastic (LVE) region in sludge. However, with the FSs in this study, the LVE region contracted to about 1% strain. This could be attributed to the anaerobic nature of the FSs, the reduced TB-EPS content, and the absence of coagulation or flocculation treatments. This is a significant reduction compared to the nearly 20% strain observed in other high-TS aerobic sludges, which also increased the sludge's sensitivity to shear [57,58].
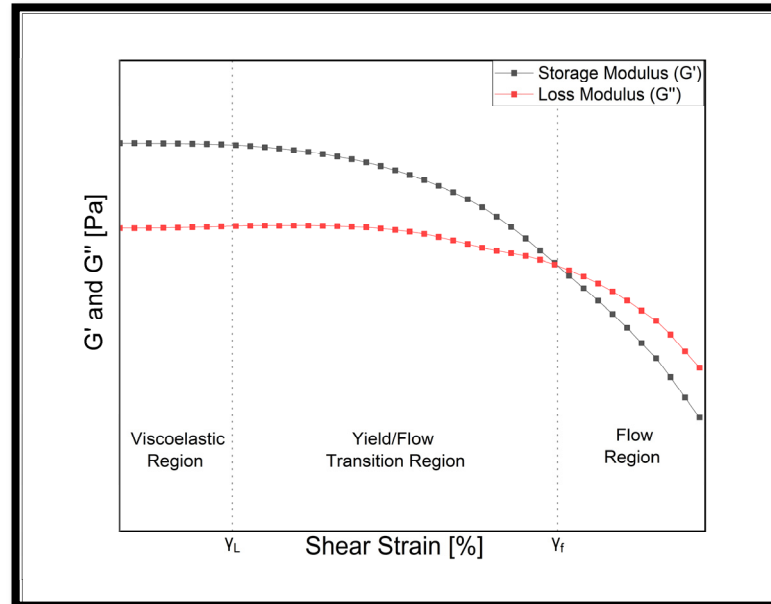


**Figure 5.** Experimental shear strain curve.

At the intersection point of $G'$ and $G''$, defined as the dynamic yield stress ($\gamma F$) or flow point, the microstructure of the high-TS VIP and UDDT sludges were strong enough to overcome any instable occurrence, such as sedimentation. Further, the higher $G''$ values indicated good elastic behaviour and spatial network structures. The increase in $G''$ may have been due to the disruption in the EPS network structure by anaerobic conditioning and the release of interstitial moisture at higher strain amplitudes. This was also observed by [57] for sludges treated by acidification and anaerobic mesophilic digestion.

Since $G' > G''$ for all samples, they were classified as viscoelastic gels, meaning they behaved as viscoelastic solids under the measurement conditions used in the test. The mean values of $G'$, LVE, and flow point for all the studied samples are shown in Table 4.

**Table 4.** Yield stress and flow point of FSs.

|  | Yield Stress | | Flow Point | |
|---|---|---|---|---|
|  | Gamma (%) | G′ (pa) | Gamma (%) | G′ (Kpa) |
| VIP | 0.031 | 47,000 | 71.772 | 133 |
| UDDT | 0.027 | 192,000 | Out of range | |

At a lower TS, sludge behaves like a diluted suspension and can be analysed using a classical rotational rheometer. There is enough moisture to fill the voids between the sludge particles, and the moisture has a lubricating effect on the motion of the solid particles. As the TS exceeds the plastic limit, the sludge can no longer be considered continuous and is more granular in nature. Thus, at a higher TS, cracks and fractures are highlighted, and this was captured during the shearing tests. This indicated the frictional interactions of

solid–solid particles, influenced by solid–liquid interactions. The sludge started to dilate, leading the solid–solid particle interactions to exhibit larger shear stresses. These frictional interactions caused dilatancy, wherein the yield stress was no longer associated with the viscous forces but rather with the frictional contacts of solid–solid particle interactions. This has been observed in pasty materials such as concrete, fresh cement, clay, etc. [45,59]. The results obtained for dilatancy are shown in Figure 6.
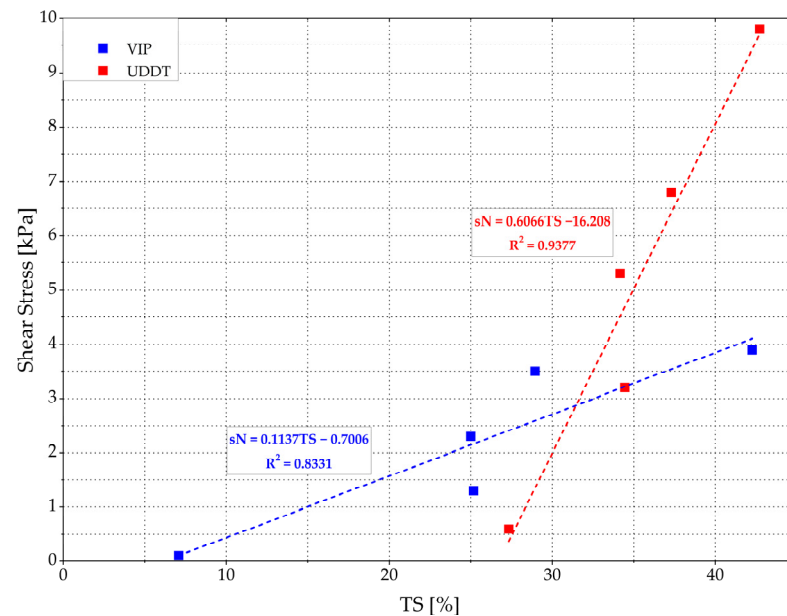


**Figure 6.** Dilatancy of VIP and UDDT sludges.

### 3.7. Filtration–Compression Cell Test

The moisture–solid particle interaction in sludges is due to the complex bio-polymeric network of mainly bacteria, resulting in a porous fractal-like structure. For highly compressible sludges, a significant quantity of moisture can be removed by filtration, especially the free moisture and some moisture occupied in the voids between the solid particles, called interstitial moisture. The characterisation of moisture distribution within the sludge provides good indicators to predict the solid–moisture interactions [60].

Among the dewaterability indices, neither capillary suction time (CST) nor specific resistance to filtration (SRF) provide either the maximum moisture removal or the type of moisture removed. Both centrifugation and a stepped pressure filtration technique can help evaluate the determination of the maximum moisture removal [61], and together with thermogravimetric analysis (TGA), the type of moisture removed can further be assessed. This approach of determining the relative contents of unbound and bound moisture fractions, and the corresponding moisture–solid binding energy, can help evaluate the sludge dewaterability [62].

The application of the stepped pressure filtration technique was adopted in the filtration–compression cell test (FCC) to help understand the moisture–solid particle interactions in the FSs, and the results can possibly be correlated to various other membrane separation technologies available for solid–liquid separability. In the FCC, a compressive piston squeezes the sludge in the direction of the filter media, and correspondingly, the filtrate is separated from the solid particles, leaving behind a sludge cake [63].

The sample height vs. pressure plot, as shown in Figure 7, provides the filtration phase as well as the expression phase. The filtration phase was linear, which was quite evident in the ST-BW sample, which had a higher initial moisture content and hence a longer filtration phase. It was during this phase that the cake formation occurred, followed by a

compression turn-up, where the cake formation ended. During the expression phase, there was movement of the solid particles within the cake structure, leading to shear stress, which became higher than it was when the sample was in suspension. This led to breakdown of weak flocs and seemed to characterise the non-traditional filtration behaviour of some sludge samples, as in the FSs. This was in accordance with the linearised filtration theory prediction of the classic "two-stage" behaviour of sludges [61], and represented the removal of moisture by cake squeezing. Several researchers have made this observation, but the results are still varied. The influence of the applied pressure on the initial sample and the final cake was not clear. The results are in good agreement with the findings by [64], and this phenomenon could be attributed to the moisture boundness of the sample, which significantly decreased with increasing pressure at the filtration phase with the release of interstitially bound moisture into unbound moisture. The transition of the filtration phase to the expression phase was smooth, and hence, it was not possible to accurately ascertain the interface.
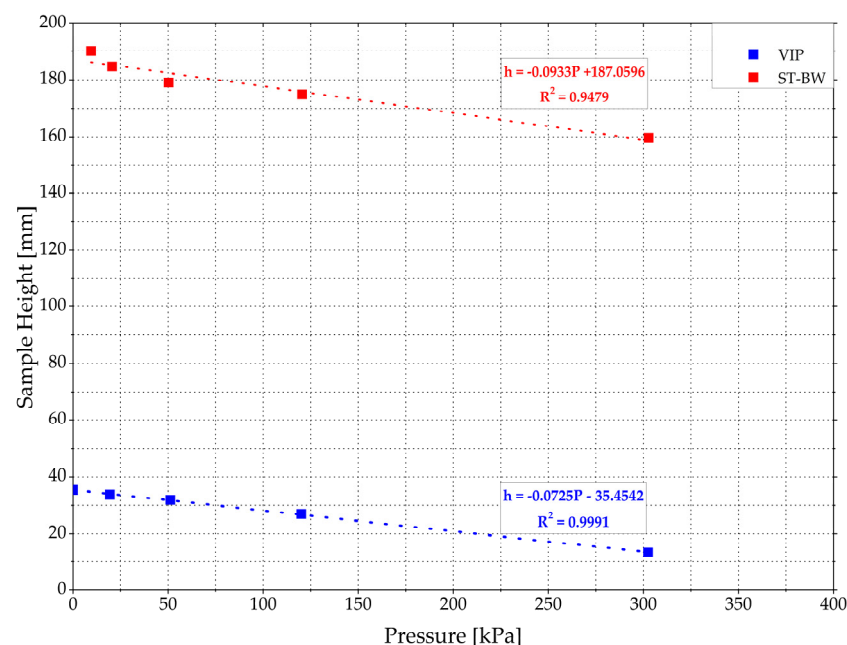


**Figure 7.** The sample height vs. pressure plot for the FS samples.

The difference in the time scale to reach the completion of the filtration phase was dramatically different, with highly extended time for the VIP compared to the ST-BW. Given that the initial TS of VIP sludge was higher than that of the ST-BW sludge, the time to reach the end of filtration should have been shorter, but it was almost an order of magnitude greater for the VIP sludge. This suggests that the VIP sludge was more compactable but had low permeability.

*3.8. Thermogravimetric Analysis*

The thermogravimetric analysis (TGA) of the raw sample and the compressed sample presented the moisture removal data (Figure 8). The slope of the TGA results provide the derivative thermogravimetric analysis (DTG) curve, which represents the rate of change in weight of the sample as a function of time [29]. From the DTG curves of the VIP and ST-BW, the rate of change in weight peaked at around the same time (7.5 min) for both sludges and for both pre-FCC and post-FCC samples. After the peak rate change, the remaining moisture in the sludge was bound moisture. Thus, the corresponding loss in weight of the moisture at the peak of the rate change provided the unbound moisture content (before the

peak), and the remaining moisture was the bound moisture content (after the peak). It was interesting to note that post compaction, there was still unbound moisture present.
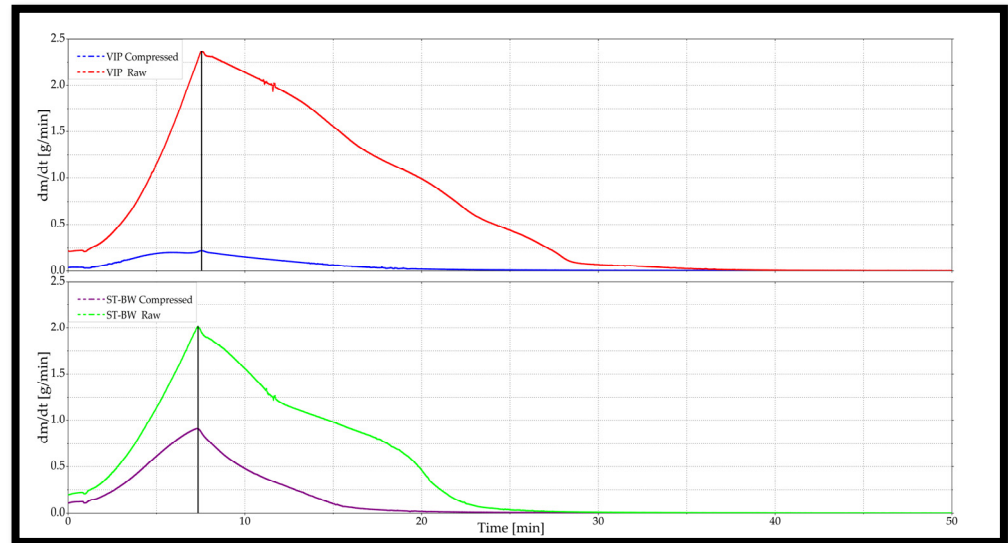


**Figure 8.** DTG curve for VIP and ST-BW pre-FCC and post-FCC.

There was significant removal of moisture in the FCC, with 36.15% of moisture removed in the VIP sludge and 47.11% of moisture removed from the ST-BW sludge. Surprisingly, a major part of this moisture was from the bound moisture, and it was mostly interstitial moisture (Figure 9). The unbound moisture reduction was 7.16–9.27%, whereas the bound moisture removal was 26.88–39.96%. This corresponded to the interstitial moisture content of the samples, which was 22.29% for VIP and 39.36% for ST-BW. The interstitial moisture from the bound moisture fraction was "pushed" out from the capillaries by the compressive force. If the compression approach of moisture removal can help remove most of the interstitial moisture, the challenges of the sticky phase of the sludge in other solid–liquid separation approaches can perhaps be overcome or reduced to a larger extent.
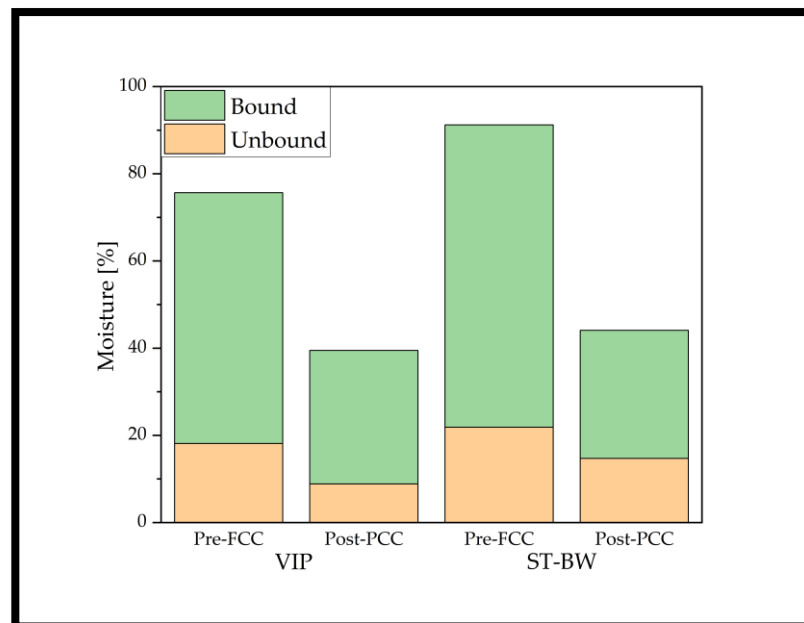


**Figure 9.** Unbound and bound moisture fractions of FSs pre-FCC and post-FCC.

### 3.9. Environmental Scanning Electron Microscopy

The environmental scanning electron microscope (ESEM) imagery at 20 μm provided details of the micro-surface of the sludge particles (Figure 10). The micro-structure of raw FS samples was heterogeneous in nature, with some degree of compactness and with some degree of porosity. The unattached particles seemed to be adhesive to the surface, demonstrating the presence of a structured EPS. The cohesive strength of the sludge was evident from the high number of active sites that aided in moisture retention and binding small grain particles. The micrograph from ESEM can be used as a reference for inevitable structural disruptions encountered in SEM methods. The sludge surface was rough, with the presence of dent-like formations. This could also have been due to the release of internal forces from the sludge surface exposed to the electron beam. This is a limitation of the ESEM approach, though not critical with sludge sample analysis. A more detailed microstructural investigation is recommended since it plays a major role in determining the deformational response of sludges to external stresses, the solid–solid particle interactions, and the resistance of sludge to shearing force [31].
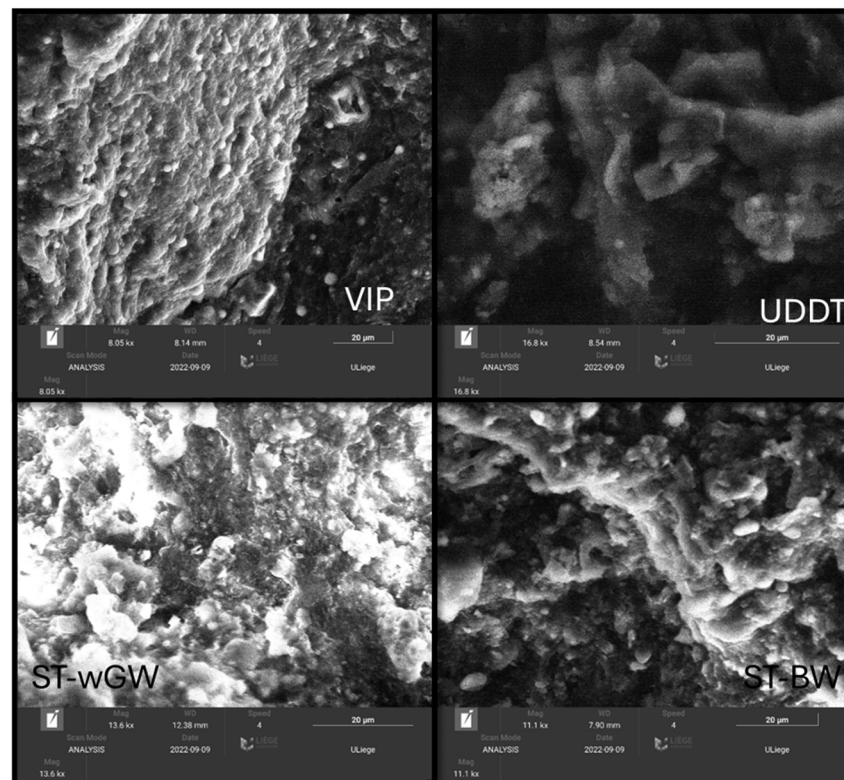


**Figure 10.** ESEM microstructural imagery of the FS samples.

## 4. Conclusions

The mechanical properties of FS and its relation to the moisture retention characteristics is significantly important to efficient sludge handling systems in the context of its treatability and land application. The FSs were largely anaerobic digested sludges with an almost stable state and without any marked biological digestion taking place. The porosity of the sludges varied between 48% to 63% for the FS samples. The true density of the FSs was lower compared with soils but was in line with the range of specific gravity of solid values of other anaerobic sludges. The zeta-potential was negative, below 10 mV and with over 95% of the particles <1000 μm. The TB-EPS influenced the stability of the sludge, with the highest being in the septic tank with the greywater sample. More proteins than carbohydrates also ascertained the anaerobic conditioning of the sludge. The results of the

textural properties using a penetrometer showed similar behaviour as that reported for sewage sludges.

The dynamic oscillatory measurements exhibited a firm but smaller linear viscoelastic behaviour of the sludges due to the change in EPS because of anaerobicity. The synchronised behaviour of $G'$ and $G''$ suggest a structural evolution from a solid characteristic to a liquid property at around the 1% strain level, fitting well with the Herschel–Bulkley model. With the application of the classical stress sweep method, with measurements from a reference value, the FS samples showed similar behaviour as that of granular materials. This helps in better understanding the flow characteristics of FS during solid–liquid separation. Compaction under a filtration–compression test resulted in the removal of both unbound and bound moisture from the sludges, reducing the moisture content of the sludge from 91.20–75.64% to 44.09–39.49% for the ST-BW and VIP sludges, respectively. The moisture removed corresponds to the interstitial moisture content of the samples. If the compression approach of moisture removal can help remove most of the interstitial moisture, the challenges of the sticky phase of sludge can perhaps be overcome or reduced to a large extent. The microstructural investigation revealed the presence of active sites that aided in moisture retention.

The moisture retention behaviour of the FSs was evidently dependent on their mechanical properties. Influencing these mechanical properties can alter this retention behaviour. While compaction can result in the release of interstitial moisture, the addition of a suitable coagulant would release vicinal moisture. Intra-cellular moisture, as observed by other researchers, can be removed only by the application of heat. It is noteworthy to observe that the moisture retention behaviour of FS can be changed by altering the mechanical properties by pre-treating the FS by different methods. The mechanical properties of FS vary depending on the initial TS concentration and the extent of anaerobic biological conditioning. While all the samples were anaerobic, the ST-wGW had very low TS and thus exhibited slightly different characteristics, while the samples from VIP and UDDT were similar, followed by ST-BW, which almost fell in the same range.

These findings provide critical insights on the influence of the mechanical properties with respect to the moisture retention behaviour of FS. Understanding these properties can assist in determining methods of effective moisture removal in FS and could pave the way for effective land applications and bioremediation. More research on the study of these mechanical properties after pre-treating can help develop a better understanding of the moisture retention behaviour and the changing patterns of moisture distribution.

**Conflicts of Interest:** The authors declare no conflicts of interest.

# References

1. Diener, S.; Semiyaga, S.; Niwagaba, C.B.; Muspratt, A.M.; Gning, J.B.; Mbéguéré, M.; Ennin, J.E.; Zurbrugg, C.; Strande, L. A value proposition: Resource recovery from faecal sludge—Can it be the driver for improved sanitation? *Resour. Conserv. Recycl.* **2014**, *88*, 32–38. [CrossRef]
2. Mallory, A.; Holm, R.; Parker, A. A review of the financial value of faecal sludge reuse in low-income countries. *Sustainability* **2020**, *12*, 8334. [CrossRef]
3. Muoghalu, C.; Semiyaga, S.; Manga, M. Faecal sludge emptying in Sub-Saharan Africa, South and Southeast Asia: A systematic review of emptying technology choices, challenges, and improvement initiatives. *Front. Environ. Sci.* **2023**, *11*, 1097716. [CrossRef]
4. Tasnim, G.; Khan, M.D.; Farooqi, I.H.; Basheer, F. Management of Wastewater and Sludge. Sources, Characteristics, Treatment Technologies and Disposal Methods for Faecal Sludge. Manag. In *Wastewater Sludge New Approaches*; Routledge: London, UK, 2023; pp. 297–337. [CrossRef]
5. Semiyaga, S.; Okure, M.A.E.; Niwagaba, C.B.; Nyenje, P.M.; Kansiime, F. Dewaterability of faecal sludge and its implications on faecal sludge management in urban slums: Faecal sludge pre-treatment by dewatering. *Int. J. Environ. Sci. Technol.* **2016**, *14*, 151–164. [CrossRef]
6. Bourgault, C.; Lessard, P.; Remington, C.; Dorea, C.C. Experimental determination of moisture sorption isotherm of fecal sludge. *Water* **2019**, *11*, 303. [CrossRef]
7. Rose, C.; Parker, A.; Jefferson, B.; Cartmell, E. The characterization of feces and urine: A review of the literature to inform advanced treatment technology. *Crit. Rev. Environ. Sci. Technol.* **2015**, *45*, 1827–1879. [CrossRef] [PubMed]
8. Gold, M.; Harada, H.; Therrien, J.-D.; Nishida, T.; Cunningham, M.; Semiyaga, S.; Fujii, S.; Dorea, C.; Nguyen, V.-A.; Strande, L. Cross-country analysis of faecal sludge dewatering. *Environ. Technol.* **2018**, *39*, 3077–3087. [CrossRef]
9. Stone, R.; Ekwue, E.; Clarke, R. Engineering Properties of Sewage Sludge in Trinidad. *J. Agric. Eng. Res.* **1998**, *70*, 221–230. [CrossRef]
10. O'kelly, B.C. Mechanical properties of dewatered sewage sludge. *Waste Manag.* **2004**, *25*, 47–52. [CrossRef] [PubMed]
11. Gold, M.; Dayer, P.; Faye, M.C.A.S.; Clair, G.; Seck, A.; Niang, S.; Morgenroth, E.; Strande, L. Locally produced natural conditioners for dewatering of faecal sludge. *Environ. Technol.* **2016**, *37*, 2802–2814. [CrossRef]
12. Blake, G.R. Bulk density. *Methods Soil Anal. Part 1 Phys. Mineral. Prop. Incl. Stat. Meas. Sampl.* **2015**, *9*, 374–390. [CrossRef]
13. Arlabosse, P.; Nzihou, A.; Oakley, S.; Sauceau, M.; Tribout, C.; Wang, F. Sludge. In *Handbook on Characterization of Biomass, Biowaste and Related by-Products*; Nzihou, A., Ed.; Springer International Publishing: Cham, Switzerland, 2020; pp. 939–1083.
14. Kuśnierz, M.; Wiercik, P. Analysis of particle size and fractal dimensions of suspensions contained in raw sewage, treated sewage and activated sludge. *Arch. Environ. Prot.* **2016**, *42*, 67–76. [CrossRef]
15. Xie, S.; Wu, Y.; Wang, W.; Wang, J.; Luo, Z.; Li, S. Effects of acid/alkaline pretreatment and gamma-ray irradiation on extracellular polymeric substances from sewage sludge. *Radiat. Phys. Chem.* **2014**, *97*, 349–353. [CrossRef]
16. Dai, Q.; Ma, L.; Ren, N.; Ning, P.; Guo, Z.; Xie, L.; Gao, H. Investigation on extracellular polymeric substances, sludge flocs morphology, bound water release and dewatering performance of sewage sludge under pretreatment with modified phosphogypsum. *Water Res.* **2018**, *142*, 337–346. [CrossRef]
17. Faye, M.C.A.S.; Zhang, K.K.; Peng, S.; Zhang, Y. Sludge dewaterability: The variation of extracellular polymeric substances during sludge conditioning with two natural organic conditioners. *J. Environ. Manag.* **2019**, *251*, 109559. [CrossRef]
18. Yang, S.-F.; Li, X.-Y. Influences of extracellular polymeric substances (EPS) on the characteristics of activated sludge under non-steady-state conditions. *Process Biochem.* **2008**, *44*, 91–96. [CrossRef]
19. Li, X.; Yang, S. Influence of loosely bound extracellular polymeric substances (EPS) on the flocculation, sedimentation and dewaterability of activated sludge. *Water Res.* **2007**, *41*, 1022–1030. [CrossRef]
20. Sheng, G.-P.; Yu, H.-Q.; Li, X.-Y. Extracellular polymeric substances (EPS) of microbial aggregates in biological wastewater treatment systems: A review. *Biotechnol. Adv.* **2010**, *28*, 882–894. [CrossRef] [PubMed]
21. Suzanne, N.S. *Food Analysis Laboratory Manual*; Springer: Berlin/Heidelberg, Germany, 2010.

22.   FAO, Quality Assurance for Animal Feed Analysis Laboratories. *FAO Animal Production and Health Manual No. 14*; FAO: Rome, Italy, 2011.

23.   Nzihou, A. *Handbook on Characterization of Biomass, Biowaste and Related By-Products*; Springer: Berlin/Heidelberg, Germany, 2020.

24.   Pambou, Y.-B. *Influence du Conditionnement et de la Déshydratation Mécanique sur le Séchage des Boues D'épuration*; Université de Liège: Liège, Belgium, 2016.

25.   Pambou, Y.; Fraikin, L.; Salmon, T.; Crine, M.; Léonard, A. Sludge dewatering and drying: About the difficulty of making experiments with a non-stabilized material. *Desalination Water Treat.* **2016**, *57*, 13841–13856. [CrossRef]

26.   Agoda-Tandjawa, G.; Dieudé-Fauvel, E.; Girault, R.; Baudez, J.-C. Using water activity measurements to evaluate rheological consistency and structure strength of sludge. *Chem. Eng. J.* **2013**, *228*, 799–805. [CrossRef]

27.   Mouzaoui, M.; Baudez, J.; Sauceau, M.; Arlabosse, P. Experimental rheological procedure adapted to pasty dewatered sludge up to 45% dry matter. *Water Res.* **2018**, *133*, 1–7. [CrossRef]

28.   Zhang, Y.; Lian, G.; Dong, C.; Cai, M.; Song, Z.; Shi, Y.; Wu, L.; Jin, M.; Wei, Z. Optimizing and understanding the pressurized vertical electro-osmotic dewatering of activated sludge. *Process. Saf. Environ. Prot.* **2020**, *140*, 392–402. [CrossRef]

29.   Deng, W.; Li, X.; Yan, J.; Wang, F.; Chi, Y.; Cen, K. Moisture distribution in sludges based on different testing methods. *J. Environ. Sci.* **2011**, *23*, 875–880. [CrossRef]

30.   Li, S.; Wang, C.; Zhang, X.; Zou, L.; Dai, Z. Classification and characterization of bound water in marine mucky silty clay. *J. Soils Sediments* **2019**, *19*, 2509–2519. [CrossRef]

31.   Lin, B.; Cerato, A.B. Applications of SEM and ESEM in microstructural investigation of shale-weathered expansive soils along swelling-shrinkage cycles. *Eng. Geol.* **2014**, *177*, 66–74. [CrossRef]

32.   Olböter, L.; Vogelpohl, A. Influence of particle size distribution on the dewatering of organic sludges. *Water Sci. Technol.* **1993**, *28*, 149–157. [CrossRef]

33.   Karczmarek, A.M.; Gaca, J. Effect of two-stage thermal disintegration on particle size distribution in sewage sludge. *Pol. J. Chem. Technol.* **2013**, *15*, 69–73. [CrossRef]

34.   Kumar, A.; Suryakumar, R.; Mercer, E.; Pocock, J.; Septien, S. Determination of Unbound-Bound Moisture Interface of Faecal Sludges from Different On-Site Sanitation Systems. *Heliyon* **2024**. [CrossRef]

35.   Cetin, S.; Erdincler, A. The role of carbohydrate and protein parts of extracellular polymeric substances on the dewaterability of biological sludges. *Water Sci. Technol.* **2004**, *50*, 49–56. [CrossRef] [PubMed]

36.   Marsalek, R. Particle size and Zeta Potential of ZnO. *APCBEE Procedia* **2014**, *9*, 13–17. [CrossRef]

37.   Comte, S.; Guibaud, G.; Baudu, M. Effect of extraction method on EPS from activated sludge: An HPSEC investigation. *J. Hazard. Mater.* **2006**, *140*, 129–137. [CrossRef] [PubMed]

38.   Peng, S.; Hu, A.; Ai, J.; Zhang, W.; Wang, D. Changes in molecular structure of extracellular polymeric substances (EPS) with temperature in relation to sludge macro-physical properties. *Water Res.* **2021**, *201*, 117316. [CrossRef]

39.   Peng, G.; Ye, F.; Li, Y. Investigation of extracellular polymer substances (EPS) and physicochemical properties of activated sludge from different municipal and industrial wastewater treatment plants. *Environ. Technol.* **2012**, *33*, 857–863. [CrossRef]

40.   Houghton, J.J.; Quarmby, J.; Stephenson, T. Municipal wastewater sludge dewaterability and the presence of microbial extracellular polymer. *Water Sci. Technol.* **2001**, *44*, 373–379. [CrossRef] [PubMed]

41.   Léonard, A.; Blandin, G.; Crine, M. Importance of Rheological Properties When Drying Sludge in a Fixed Bed. *Lab. Chem. Eng. Univ.* **2014**, *III*, 102–150.

42.   Azeddine, F.; Sergio, P.A.; Angélique, L.; El Khadir, L.; Ali, I.; El Houssayne, B. Rheological Behavior and Characterization of Drinking Water Treatment Sludge from Morocco. *Clean Technol.* **2023**, *5*, 259–273. [CrossRef]

43.   Li, B.; Wang, F.; Chi, Y.; Yan, J.H. Adhesion and Cohesion Characteristics of Sewage Sludge During Drying. *Dry. Technol.* **2014**, *32*, 1598–1607. [CrossRef]

44.   Hil, A.; Judenne, E.; Remy, M. The effect of lime treatment on sludge rheological properties. *Technology* **2005**, *59*, 1–6.

45.   Mezger, T. *The Rheology Handbook*; Vincentz Network: Hannover, Germany, 2020.

46.   Rodríguez, N.H.; Ramírez, S.M.; Varela, M.B.; Guillem, M.; Puig, J.; Larrotcha, E.; Flores, J. Re-use of drinking water treatment plant (DWTP) sludge: Characterization and technological behaviour of cement mortars with atomized sludge additions. *Cem. Concr. Res.* **2010**, *40*, 778–786. [CrossRef]

47.   Liu, Y.; Zhuge, Y.; Chow, C.W.; Keegan, A.; Li, D.; Pham, P.N.; Huang, J.; Siddique, R. Utilization of drinking water treatment sludge in concrete paving blocks: Microstructural analysis, durability and leaching properties. *J. Environ. Manag.* **2020**, *262*, 110352. [CrossRef]

48.   Dignac, M.-F.; Ginestet, P.; Rybacki, D.; Bruchet, A.; Urbain, V.; Scribe, P. research, and undefined. In *Fate of Wastewater Organic Pollution During Activated Sludge Treatment: Nature of Residual Organic Matter*; Elsevier: Amsterdam, The Netherlands, 2000.

49.   Ling, Y.P.; Tham, R.-H.; Lim, S.-M.; Fahim, M.; Ooi, C.-H.; Krishnan, P.; Matsumoto, A.; Yeoh, F.-Y. Evaluation and reutilization of water sludge from fresh water processing plant as a green clay substituent. *Appl. Clay Sci.* **2017**, *143*, 300–306. [CrossRef]

50. Li, H.; Zou, S.; Li, C. Liming Pretreatment Reduces Sludge Build-Up on the Dryer Wall during Thermal Drying. *Dry. Technol.* **2012**, *30*, 1563–1569. [CrossRef]

51. Léonard, A.; Royer, S.; Blandin, G.; Salmon, T.; Fraikin, L.; Crine, M. Importance of Mixing Conditions During Sludge Liming Prior to Their Convective Drying. In Proceedings of the EuroDrying'2011: III European Drying Conference, Palma de Mallorca, Spain, 26–28 October 2011; pp. 26–28.

52. Huron, Y.; Salmon, T.; Crine, M.; Blandin, G.; Léonard, A. Effect of liming on the convective drying of urban residual sludges. *Asia-Pac. J. Chem. Eng.* **2010**, *5*, 909–914. [CrossRef]

53. Benlalla, A.; Elmoussaouiti, M.; Cherkaoui, M.; Ait Hsain, L.; Assafi, M. Characterization and valorization of drinking water sludges applied to agricultural spreading. *J. Mater. Environ. Sci.* **2015**, *6*, 1692–1698.

54. Malkin, A.Y.; Derkach, S.R.; Kulichikhin, V.G. Rheology of Gels and Yielding Liquids. *Gels* **2023**, *9*, 715. [CrossRef] [PubMed]

55. Ruiz, T.; Wisniewski, C. Correlation between dewatering and hydro-textural characteristics of sewage sludge during drying. *Sep. Purif. Technol.* **2008**, *61*, 204–210. [CrossRef]

56. Jiang, J.; Wu, J.; Poncin, S.; Li, H.Z. Rheological characteristics of highly concentrated anaerobic digested sludge. *Biochem. Eng. J.* **2014**, *86*, 57–61. [CrossRef]

57. Zhang, S.; Liang, J.; Huang, J.; Huang, S.; Zheng, L.; Sun, S.; Zhong, Z.; Zhang, X.; Yu, X.; Guan, Z. Analysis of the relationship of extracellular polymeric substances to the dewaterability and rheological properties of sludge treated by acidification and anaerobic mesophilic digestion. *J. Hazard. Mater.* **2019**, *369*, 31–39. [CrossRef] [PubMed]

58. Feng, G.; Hu, Z.; Ma, H.; Bai, T.; Guo, Y.; Hao, Y. Semi-solid rheology characterization of sludge conditioned with inorganic coagulants. *Water Sci. Technol.* **2019**, *80*, 2158–2168. [CrossRef] [PubMed]

59. Sollich, P. Soft Glassy Rheology. In *Molecular Gels*; Weiss, R.G., Terech, P., Eds.; Springer: Dordrecht, The Netherlands, 2006. [CrossRef]

60. Vaxelaire, J.; Olivier, J. Conditioning for municipal sludge dewatering. From filtration compression cell tests to belt press. *Dry. Technol.* **2006**, *24*, 1225–1233. [CrossRef]

61. Scales, P.; Dixon, D.; Harbour, P.; Stickland, A. The fundamentals of wastewater sludge characterization and filtration. *Water Sci. Technol.* **2004**, *49*, 67–72. [CrossRef] [PubMed]

62. Wu, B.; Dai, X.; Chai, X. Critical review on dewatering of sewage sludge: Influential mechanism, conditioning technologies and implications to sludge re-utilizations. *Water Res.* **2020**, *180*, 115912. [CrossRef] [PubMed]

63. Raynaud, M.; Vaxelaire, J.; Olivier, J.; Dieudé-Fauvel, E.; Baudez, J.-C. Compression dewatering of municipal activated sludge: Effects of salt and pH. *Water Res.* **2012**, *46*, 4448–4456. [CrossRef]

64. Raynaud, J.-C.; Vaxelaire, M.; Heritier, J.; Baudez, P. Activated sludge dewatering in a filtration compression cell: Deviations in comparison to the classical theory. *Technology* **2009**, *7*, 743–753. [CrossRef]